27th EPS Conference on Contr. Fusion and Plasma Phys. Budapest, 12-16 June 2000 ECA Vol. **24B** *(2000) 1248 -1251*

The search for topological structures in TJ-II radiation profiles using an automated pattern recognition procedure

A. Baciero, B. Zurro, K.J. McCarthy, A. López-Fraguas, J. Vega, C. Cremy, C. Burgos and TJ-II Team

Laboratorio Nacional de Fusión, Asociación Euratom-CIEMAT, E-28040 Madrid, Spain

Introduction. Significant features have been observed in impurity line emission or bremsstrahlung profiles obtained in stellarator [1] and tokamak [2,3] devices using fast spectroscopic scanning systems having high spatial resolution. Such features, which consist of flats and humps, provide evidence for the existence of topological structures in plasma interiors. It has been postulated that such structures arise as a result of perturbations in electron temperature and ion density profiles caused by magnetic islands. Due to the good conduction along field lines, islands may be expected to show up in temperature and pressure profiles, and consequently in impurity radiation profiles. Effects associated with low-order magnetic islands have been seen in several tokamaks and for several techniques. As yet, studies of topological structures in stellarator plasmas are less extensive. For the TJ-II flexible heliac [4], we have continued with the approach initiated in the TJ-IU torsatron, and we have designed and optimised an experimental system. In addition, we have developed a numerical algorithm for studying this problem. Here, we describe both the experimental apparatus and the pattern recognition algorithm developed to analyse data. Finally, we present the results of an analysis made on profiles from ECR heated plasmas in the TJ-II.

Experimental. The measurements reported here were made on plasmas heated by electron cyclotron waves with total injected power values from 300 to 600 kW. A wide range of rotational transforms is possible on this device, i.e., $0.14 < \iota(0) < 0.3$. Provided that the value of the rotational transform is well removed from low order rationals, closed nested magnetic surfaces are present. Otherwise large islands are observed. Plasmas with maximum line-averaged electron densities of 1.1×10^{19} m^{-3} and central electron temperatures of 1 keV were used for this experiment. Chord-integrated C V (227.1 nm) line emission profiles were obtained using a 0.5 m focal length monochromator based system. The plasma was viewed from above its outer equatorial plane, as shown in Fig.1a, and the monochromator system was positioned, as shown in Fig. 1b, with respect to the scanning mirror pivotal point. The spatial resolution and sensitivity were maximised for these measurements by imaging the optical radiation along the entrance slit of the monochromator using only a scanning mirror and lens

located above this slit. For this, the input slit height (5 mm) is focused along the plasma toroidal direction, while the width (250 μm) multiplied by the ×10 optical magnification fixes the poloidal resolution. This set-up has several advantages, in particular, it is not necessary to rotate the image, the number of optical components required is minimised while the resultant spatial resolution is maximised. Furthermore, by placing a flash lamp at the second focal plane, which can be selected by folding away the auxiliary mirror, indicated here by an arrow, optical alignment of the whole system is made easier. The fast rotating polygonal mirror (six faces) allows the plasma minor diameter to be scanned in about ~1 ms once every 10 ms. This allows us to repeatedly scan the plasma (top to bottom) along a typical 300 ms discharge. Finally, signals from the photomultiplier tube mounted at the primary focal plane were shaped by a current amplifier (bandwidth=200 kHz, gain=10^6 V/A) and the output signals were digitised every microsecond by a dedicated CAMAC data acquisition system (12 bits).

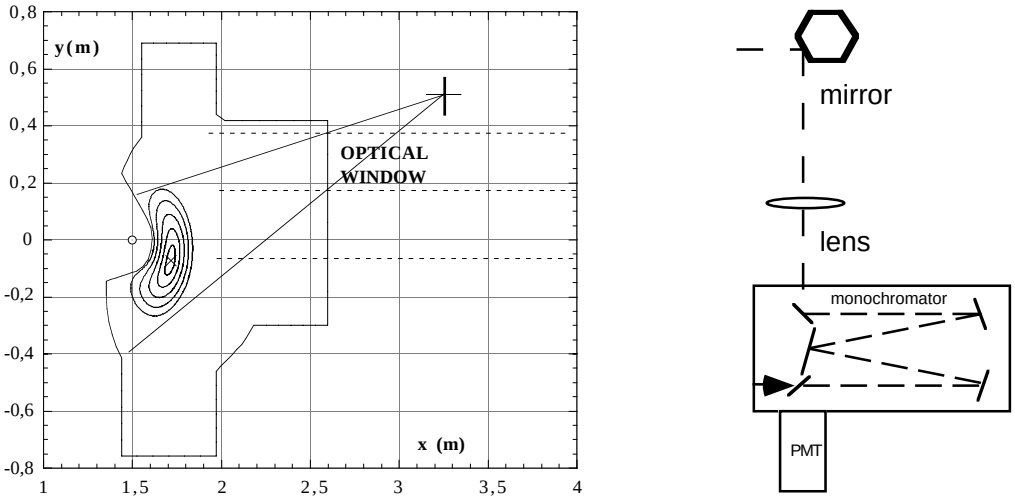

Fig. 1. a) A sketch of the plasma observation geometry indicating the pivotal point of the scanning mirror (+), the quartz optical window, the plasma and the chamber geometry; b) a scheme of the spectrometer and optics used to obtain impurity line profiles.

Pattern recognition algorithm. The algorithm begins by smoothing (multi-point averaging) and filtering (low, band, or high pass) the profiles recorded along a discharge in order to reduce some of the disturbances caused by fluctuations and electronic noise. Next, a cross-correlation technique is used to deduce the repetition period between profiles and to correct for even small changes introduced in this period caused by variations in the configuration or inaccuracies in the scanning system. The first profile within a selected set (sets contain 18

profiles in the discharges analysed here) is used to determine the profile centre and the location times required by the algorithm for referencing the locations of the features found. Then, beginning at the centre of each profile, it searches for flats and humps and classifies these in a table according to their relative location. Those that occur within the spatial resolution of the measurement system are assigned to the same topological feature. Two free parameters are used here for including a feature in the table. These are its width and the relative slope variation. Before providing a summary of the features found within the discharge, the condition applied to a feature is that its frequency of apparition is greater than a predetermined value, typically 40 %. It is also possible to identify the most prominent features by varying this value. Finally, by imposing the restrictive constraint that features should be symmetric about the profile centre in order to be associated with an island chain (at least over a significant number of samples), the possibility of fluctuations jeopardising the procedure is minimised.

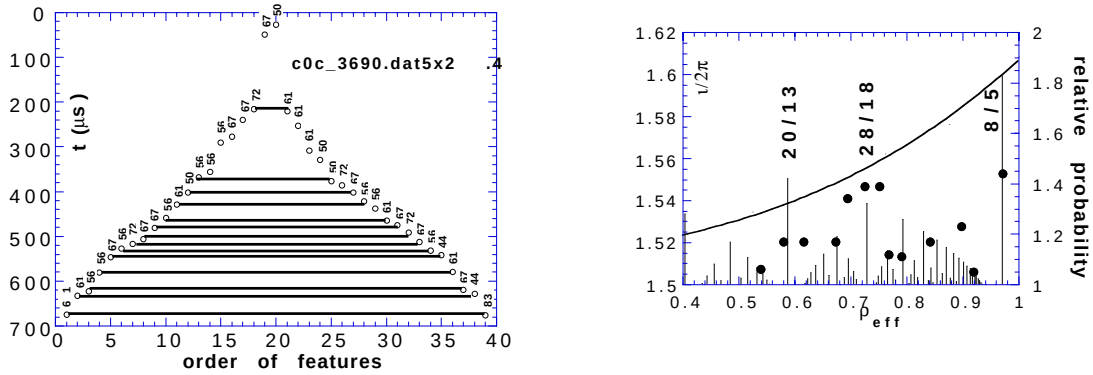

Fig. 2. a) Plot of location (in time), with respect to profile centre, of flats and humps occurring in a set of discharge profiles (when scanning from top to bottom). Only features that occur repeatedly in >40% of profiles of the set are included; b) Symmetric features in a) are converted to effective plasma radius and compared with the theoretical positions of the most relevant iota resonances.

First results. After optimising the experimental system and developing a preliminary version of the algorithm, it was applied to a selected group of discharges corresponding to the standard TJ-II magnetic configuration 100_40_63. Results of the analysis made on the TJ-II discharge #3690 are shown in Fig. 2. Here, the y-axis of Fig. 2a represents displacement from the profile centre (in microseconds) while the x-axis gives the identification number of a feature provided by the algorithm when analysing the profiles under a fixed set of analysis conditions and running sequentially from the plasma top to bottom. In Fig 2b, these

symmetric positions are converted to flux co-ordinates and they are plotted together with the theoretical iota profile. Also, the positions of some of the most important rational surfaces are indicated by vertical lines, whose heights represent island width. On the right y-axis, the relative probability of finding a feature in the18 profiles of the same discharge is plotted. Indeed, the coincidence between the experimental measurements and the most significant rational surfaces is good. A similar but more statistical relevant analysis has been performed by combining 6 successive discharges (#3686-#3691) and the results are plotted in Fig. 3. In this case, the condition of symmetry has not been enforced, however, the frequency of appearance on both sides is used as a weighting when calculating the relative probability plotted in this figure.

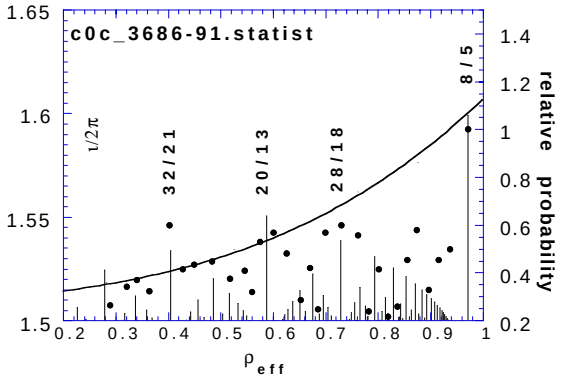

Fig. 3. Plot of features detected in a statistical analysis of 6 discharges. The most relevant resonances deduced from the theoretical iota profile are indicated and vertical lines represent resonance positions.

Acknowledgements. This work was partially funded supported by the Spanish Ministry of Education under Project PB97-0160. A. B. is supported by a Scholarship from the Institute of Energy Studies.

References

[1] B. Zurro, K. J. McCarthy, E. Ascasíbar, F. Aragón, C. Burgos, A. López and A. Salas, *Europhys. Lett.* 40 (1997) 269-274.

[2] Vershkov V. A., Krupin V. A., Pimenov A. B. and Khvostenko P. P., *Sov. J. Plasma Phys.* 10 (1984) 515.

[3] Zurro B. and García-Castañer B., *Rev. Sci. Instrum.* 65 (1994) 2580.

[4] Alejaldre C. and TJ-II Team, Plasma Phys. Control. Fusion 41 (1999) B109.